Earthquake Engineering, Tenth World Conference © 1992 Balkema, Rotterdam. ISBN 90 5410 060 5

A study on damping effect of dissipation energies by viscous damping and hysteresis loop on earthquake responses

M. Kibayashi & T. Hisatoku
Takenaka Corporation, Osaka, Japan

T. Nagano, T. Kitano, H. Yoshida & M. Ohue
The Kansai Electric Power Co., Inc., Osaka, Japan

ABSTRUCT: The object of this paper is to investigate the vibrational damping effects of the shear wall structures caused by the energy dissipation of the viscous damper *h* and the plastic hysteresis loop under strong earthquakes.

It is revealed through analytical study using single degree of freedom systems of Reversed-S hysteresis model,which has the property to keep at the constant equivalent viscous damping ratio *he*, that the plastic hysteresis dissipated energy ratio *Ep / Et* is increased steeply as the ductility factor response increased, and converged to the ratio of the plastic energy dissipation capacity to the total capacity *heq / (h+heq)*. Consequently, it is found that the substitute damping ratio *he* is expressed in the same manner as that described for the plastic dissipated energy ratio, and is converged to the total capacity composed of viscous damper and plastic hysteresis loop *h+heq*.

1 INTRODUCTION

In practical earthquake response analysis of the building structures, a lumped mass system composed of the Voigt type mechanical model is commonly used.

The properties of the mass and the stiffness components are estimated definitely by means of the structural calculations and the analytical procedures.

On the other side, there is almost no theoretical explanation about the damping characteristics. In general, the following mechanism of vibrational damping can be listed, (1) internal friction, (2) external friction, (3) sliding friction, (4) plastic hysteresis, and (5) wave radiation through soil media. It is impossible to make clear the contribution of these factors definitely, so that the damping mechanism is estimated looking upon as the comprehensive viscous damper in usual practice.

Among these factors, the plastic energy dissipation of the structural members takes an important role in the vibrational damping effects under strong earthquake motions, and Jacobsen (1960) proposed the concept of equivalent viscous damping ratio *heq* to the hysteretic type of damping.

The analytical study of Gulkan and Sozen (1974) made it clear that the substitute damping ratio of reinforced concrete frame is a function of the ductility factor, using Takeda's hysteresis model. They proposed the concept of the substitute damping related to hysteretic energy dissipation property, as a part of the study on the simplified method for estimating the design base shear taking account of inelastic response.

However, the inelastic behavior of the reinforced concrete shear walls is different from the reinforced concrete frames, and has direct effect upon earthquake responses, as pointed out by Shiga et al. (1974).

According to the recent experimental study on the shear walls applied to the nuclear power plant buildings, it is reported by Inada (1987) that the restoring force characteristics of the shear wall has the properties that the shape of the plastic hysteresis loop contains the slip deformation, and the equivalent viscous damping ratio has a tendency to keep at a constant value independent of the plastic deformation. It is also proposed that the restoring force skeleton curve can be expressed in the form of trilinear curve to the shear deformation component τ - γ.

The authors have proposed in 1984 that it is reasonable to apply Reversed-S hysteresis (R-S) model to shear wall structures, because of the plastic energy dissipation.

As concerning with a dynamical experiment of reinforced concrete shear wall structures, it is reported by Setogawa and Yano et al. (1988) that the damping ratio is of 1 - 2 % to critical on the small vibration range, but is increased corresponding to the input level, and reached up to the ratio of 4 - 6% on near the ultimate state. These studies were carried out through the large scale shaking table test of the scaled shear wall structures applied to nuclear power plant buildings, subjected artificial earthquake with intensity ranging from the elastic linear state up to the ultimate state.

This paper presents the vibrational damping effects of shear wall structures caused by the dissipated energy of viscous damper and plastic hysteresis loop under strong earthquake motions.

Analytical study using the single degree of freedom (SDOF) pendulum is carried out, in order to investigate the inelastic response characteristic of R-S model on comparing with another conventional hysteresis model.

The energy distribution characteristics to the viscous damper and the plastic hysteresis loop is studied in more detail, so that the relative relation between the initial viscous damping ratio and the equivalent viscous damping ratio of hysteresis loop is investigated. Subsequently, the characteristics of substitute damper with reference to Gulkan's report is demonstrated from the view point of the energy dissipation capacity.

Moreover, in order to examine the application of the results of SDOF systems to multi-degrees of freedom (MDOF) systems, analytical study by the 5-DOF pendulum is carried out further.

2 ANALYSIS MODELS

2.1 *Reversed-S hysteresis model*

R-S model has the following characteristics.

1) The unloading stiffness from the plastic process is deteriorated.

2) The slip deformation is occurred at low level load Qs after the unloading process.

The slip process pass through the constant point Qc at zero deformation, which is assumed to be the same with slip load on the opposite side.

3) The hardening deformation is occurred after the slip process at higher load QH than the slip load.

4) The equivalent viscous damping ratio *heq* has a tendency to keep at a constant value independent of plastic deformation.

The characteristics points Qs and QH are set to be $0.125\ Qy1$ and $0.25\ Qy1$, respectively, so as to get the equivalent viscous damping ratio to be 5 %.

2.2 *Single degree of freedom systems*

The SDOF pendulum composed of constant mass *m*, viscous damper *co* and inelastic stiffness *k(D)* on fixed base condition is used, as shown in Fig.1.

From the view point of energy dissipating capacity composed of the viscous damper and the plastic hysteresis loop, distribution ratio between initial viscous damping ratio *h* and equivalent viscous damping ratio *heq* is mainly investigated.

The dynamic properties of the models are set by considering the practical application, as follows.

1) Input earthquake motions : Three accerelogram records of the strong earthquake motion of El Centro 1940 NS, Taft 1952 EW and Hachinohe 1968 NS digitalized by Building Center of Japan are used. The acceleration response spectra of these motions are shown in Fig.2.

2) Input level *AI*: Five levels of input amplitude of 1.0, 1.5, 2.0, 3.0 and 4.0 *Aiy1* are used, with intensity ranging from the yield to the ultimate state. The input amplitude ratios are expressed in the values relative to the input acceleration when structure reaching to the yield strength *Aiy1*

3) Natural periods *T* : Five natural periods of 0.2, 0.4, 0.6, 0.8 and 1.0 sec. are used. These periods are corresponding to the constant acceleration range and constant velocity range on the input motions' response spectra.

4) Viscous damping ratio *h* : Two viscous damping ratios of 3 % and 1 % to critical are used. From the view point of energy dissipating capacity , the viscous damping capacity is considered as a variable.

5) Plastic hysteresis model : Three hysteresis of R-S, Peak-Oriented (P-O) and Normal Trilinear (N-Tri) models, as shown by Umemura et al.(1973), are used considering the plastic hysteresis energy dissipation capacity. R-S model has a property to keep at a constant dissipation capacity, P-O model neglects the

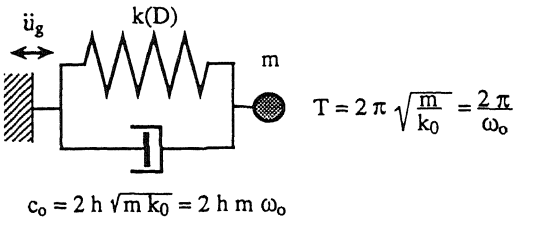

(a) Mechanical model

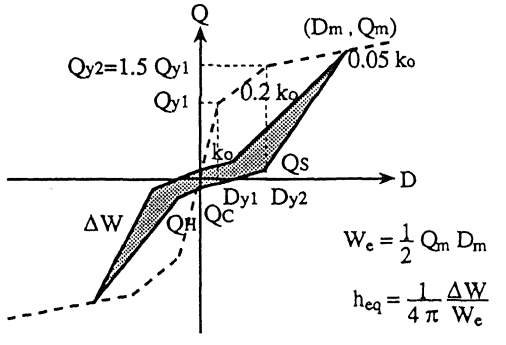

(b) Reversed-S restoring force model

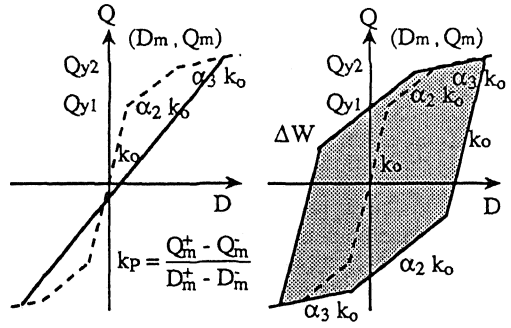

(c) Conventional hysteresis loop models

Fig.1 Single degree of freedom model

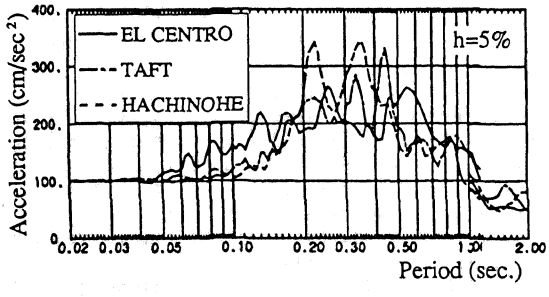

Fig.2 Response spectra of input motions

hysteretic energy dissipation, and N-Tri model is the upper limit of the plastic energy dissipation capacity.

The restoring force skeleton curve and the equivalent viscous damping ratio of the R-S model are set to the trilinear model and to be 5 %, with reference to Inada's report, as shown in Fig.1.

On investigating the effect of hysteresis models, the analytical parameters of natural periods are limited to 0.2, 0.4 and 0.8 sec., and the viscous damping ratio is limited to 3 %.

The parameter of the hysteresis model on studying the energy dissipation characteristics is limited to R-S model.

2.3 *Multi-degrees of freedom systems*

The 5-DOF pendulum which has the equivalent dynamic properties to the SDOF system is used.

The dynamic properties of the 5-DOF models are set to have uniform mass and parabolic stiffness distribution, as shown in Fig.3. The modal damping ratio at higher order is conventionally fixed at a constant value independent of the vibrational frequency. The stiffness distribution is set to be in triangular shape of the first mode. The yield strength distribution is similar to that of stiffness, but is adjusted linearly at the top story, so that the yield begins at the first story.

On investigating the effect of MDOF systems, the analytical parameters are limited based on the results of SDOF systems. The input motion is El Centro 1940 NS. The natural periods are 0.2, 0.4 and 0.8 sec. The viscous damping ratio is 3 %, and the hysteresis model is R-S model.

3 VIBRATIONAL DAMPING EFFECTS

3.1 *Effects of plastic hysteresis models*

The analytical results concerning with the effect of hysteresis characteristics on the earthquake responses are shown as follows.

1) The maximum acceleration responses A / A_{y1} corresponding to the input level are shown in Fig.4, in the case of El Centro input motion and natural period of 0.2 sec.

It is observed that the maximum responses of R-S model are slightly less than that of P-O model, but much greater than that of N-Tri model.

The maximum responses of R-S model have similar features to P-O model in short periods. However, the responses of R-S model have different features in strong input levels or long periods to be considerably less than that of P-O model, caused by the plastic energy dissipation capacity.

It is clearly shown that the plastic hysteresis energy dissipation take an important role in the vibrational damping effect.

2) The total input energy ratio E_I / E_{Iy1} in relation to the input level is shown in Fig.5, in the case of El Centro input motion.

The total input energy is increased exponentially in proportion with the input level.

It has a remarkable tendency to be in the same degree in spite of the difference of the hysteresis model, as pointed out by Akiyama and Kato (1975).

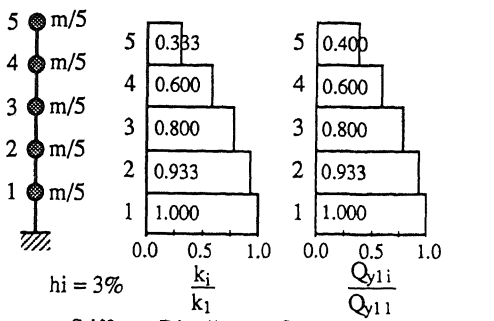

Fig. 3 5-degrees of freedom model

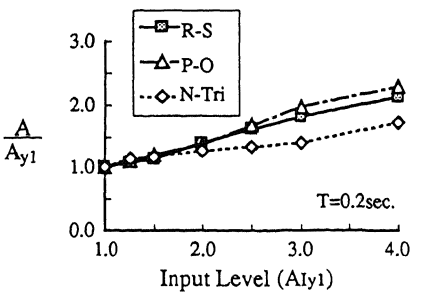

Fig.4 Maximum acceleration responses (El Centro)

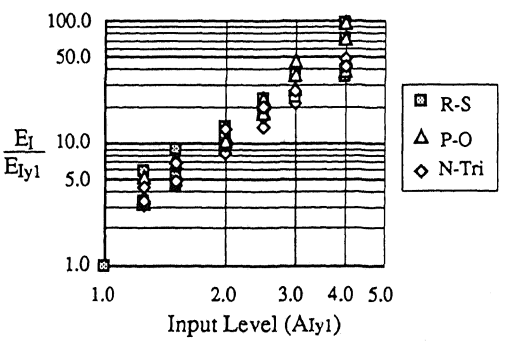

Fig.5 Total input energy responses (El Centro)

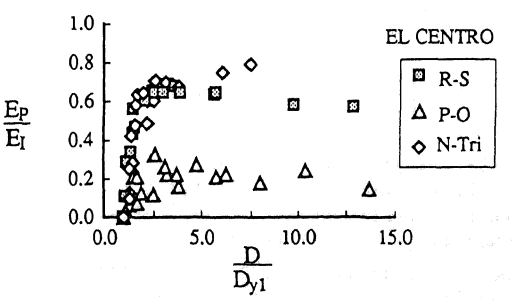

Fig.6 Ratios of total plastic energy to input energy

3) The ratio of the plastic hysteresis dissipated energy to the total input energy E_P / E_I in relation to the ductility factor response is shown in Fig.6, in the case of El Centro input motion.

The plastic energy dissipation ratio of R-S model is observed to increase linearly from zero, and approaches to the fixed value of 60% near the ductility factor of 3. After this bending point, the ratio keeps at a constant value.

On the other hand, the plastic energy dissipation ratio of N-Tri model has a tendency to increase more after the bending point, but the gradient become slow.

It becomes clear that the plastic energy dissipation capacity of R-S model is limited, because the equivalent viscous damping ratio of the hysteresis loop keeps at a constant value independent of the plastic deformation.

4) The relation between the plastic hysteresis dissipated energy E_P and the plastic work W_P is shown in Fig.7.

These values are expressed in values relative to the potential energy at yield level $W_{yl} = Q_{yl} D_{yl} / 2$.

The plastic work is represented by the area under the skeleton curve at the maximum response on both positive and negative side.

It is observed that the plastic dissipated energy of R-S model is in linear proportion to the plastic work.

The hysteresis path of R-S model has a remarkable tendency to expand over the previous maximum process, while N-Tri model path makes a loop accumulatively within the narrow range.

3.2 *Energy dissipation characteristics*

On the basis of the previous results concerning with the restoring force hysteresis effects, the energy distribution characteristics of the total input energy to the viscous damper and the plastic hysteresis loop is studied in more detail.

In order to simplify the effect of plastic energy dissipating capacity, R-S model is used, because of the property of constant equivalent viscous damping ratio.

These distribution factors are represented with the relation of the ductility factor response, so as to exclude the effect of the input motions and natural periods.

For the purpose of estimating the comprehensive damping effect, the substitute damper is used. The damping ratio of substitute damper he, which is at the equivalent dissipating capacity to the total input energy of the inelastic structure, is derived from equation (1) with reference to Gulkan's report.

$$h_e = \frac{1}{2 m \omega_o} \frac{E_I}{\left(\frac{E_D}{c_o}\right)} \qquad (1)$$

$$E_I = m \int_0^t \ddot{u}_g \dot{u} \, dt \,, \; E_D = c_0 \int_0^t \dot{u}^2 \, dt$$

On this equation, it is assumed that the energy dissipation procedure of substitute damper is in the same manner as that of the inelastic structure, so that these energies are estimated by the value of the integral of input acceleration $\ddot{u}_g$ and/or relative response velocity $\dot{u}$ of the inelastic system over the time duration of input motion.

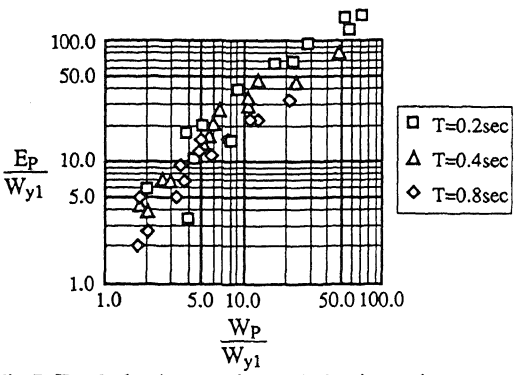

Fig.7 Total plastic energies and plastic works

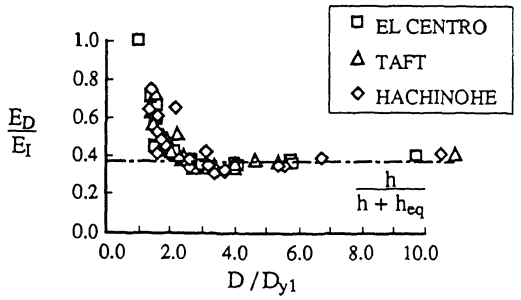

(a) Viscous damper dissipated energy ratios

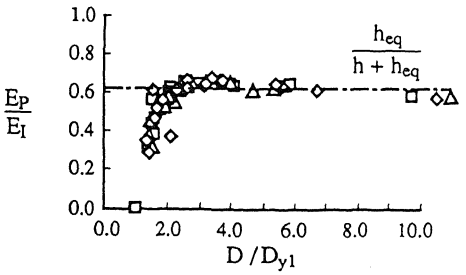

(b) Plastic hysteresis dissipated energy ratios

Fig.8 Energy distribution factors in case of h = 3%

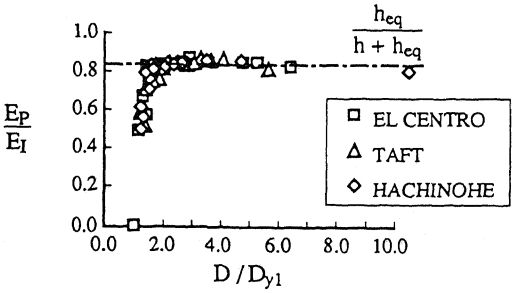

Fig.9 Plastic energy ratios in case of h = 1%

Furthermore, in order to estimate the dissipating energy capacity, substitute damping ratio *he* is related to the damping coefficient c_e through the coefficient *m* and ω_o, in the same manner as the relation between the viscous damping ratio *h* and damping coefficient c_o of inelastic structures.

1) The ratios of the viscous damper dissipated energy and the plastic hysteresis dissipated energy to the total input energy, are shown in Figs.8 and 9, corresponding to the initial viscous damping ratios, respectively.

The viscous damper dissipated energy ratio E_D / E_I is observed to be decreased hyperbolically as the ductility factor increased, and approached to the fixed values of about 40 % and 15 % corresponding to the initial viscous damping ratios 3 % and 1 %, respectively.

These converged ratios agree well with the ratios of viscous damping capacities to total damping capacities composed of the viscous damper and the plastic hysteresis loop $h / (h+he)$.

While, the plastic dissipated energy ratio E_P / E_I is increased complementarily, as mentioned above.

2) The substitute damping ratios expressed in values relative to the initial viscous damping ratios are shown in Figs.10 and 11, corresponding to the initial viscous damping ratios 3 % and 1 %, respectively.

The substitute damping ratio is observed to be increased steeply and approached to the fixed value, in the same manner as the plastic dissipated energy ratio.

The converged values are 2.7 and 6.0 corresponding to the initial viscous damping ratios 3 % and 1 %, respectively. These values agree well with the sum of initial viscous damping ratio and equivalent viscous damping ratio of the hysteresis loop $(h+he) / h$.

Consequently, it is concluded clearly that the substitute damping ratio *he* is increased linearly from the initial viscous damping *h* at the beginning of the plastic range, and is converged to the sum of the viscous damping capacity and equivalent viscous damping capacity $h+heq$ near the ductility factor of 3.

3.3 *Applications to multi-degrees of freedom systems*

The energy distribution characteristics of the 5-DOF pendulum with equivalent dynamic properties to the SDOF systems are shown here.

1) The maximum acceleration response comparing with the equivalent SDOF system is shown in Fig.12, and the distribution shapes of the ductility factor is shown in Fig.13.

It can be seen that the maximum responses of accelerations at the top story A_{Top} and total sway angles $\gamma_{Top} = D_{Top} / H_{Whole}$ are in good agreement with the equivalent SDOF system.

However, the distribution shapes of the ductility factor varies as the input level increase, and have a tendency to concentrate the plastic damage to the lower story.

2) The viscous damper dissipated ratio and the plastic hysteresis dissipated ratio are shown in Fig.14.

The energy distribution factors also agree well with the equivalent SDOF system, in spite of the difference of the ductility factor responses in each story.

3) Consequently, the substitute damping ratio of 5-DOF systems is expressed in the same manner as that described for SDOF systems, as shown in Fig.15.

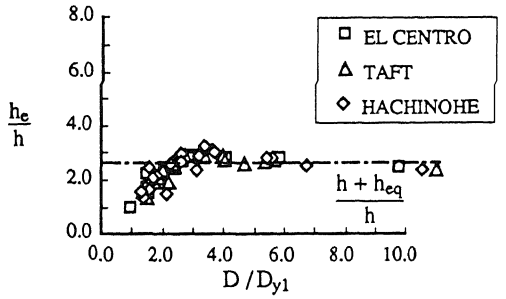

Fig.10 Substitute damping ratios in case of h = 3%

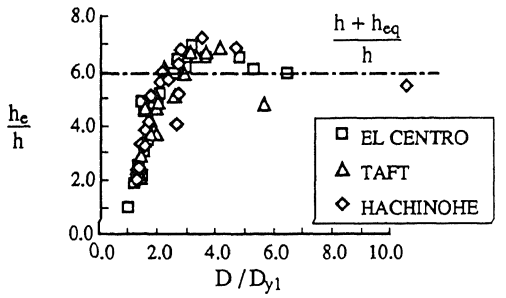

Fig.11 Substitute damping ratios in case of h = 1%

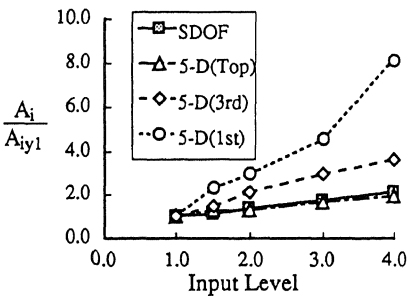

Fig. 12 Maximum acceleration reponses (5-DOF)

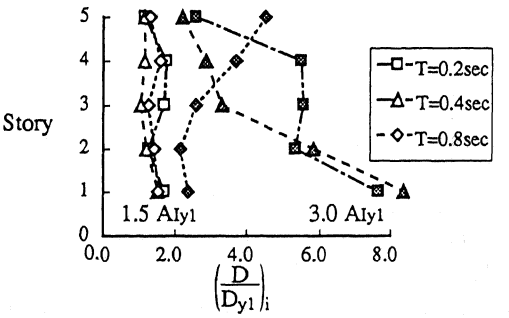

Fig. 13 Maximum ductility factor reponses (5-DOF)

4 CONCLUSIONS

Analytical studies on vibrational damping effects of the reinforced concrete shear wall structures by the energy dissipation of the viscous damper and the plastic hysteresis loop derive the following concluding remarks.

1) The maximum responses of R-S model are less than that of P-O model rationally, but much greater than N-Tri model, caused by the plastic energy dissipating capacity.

2) It becomes clear that the plastic hysteresis dissipated energy ratio is increased steeply as the ductility factor increased, and converged to the ratio of plastic dissipating capacity to the total dissipating capacity composed of damper and plastic hysteresis loop *heq/(h+heq)*, because the equivalent viscous damping ratio of R-S model keeps at a constant value and hysteretic dissipating capacity is limited.

3) It is found that the substitute damping ratio *he* is increased in the same manner as the plastic dissipated energy ratio, and is converged to the sum of the dissipating capacity of viscous damper and plastic hysteresis loop *h+heq*.

4) In the case of the strength distribution shape being similar to that of stiffness, it is confirmed that the the results of SDOF systems are applied well to MDOF systems.

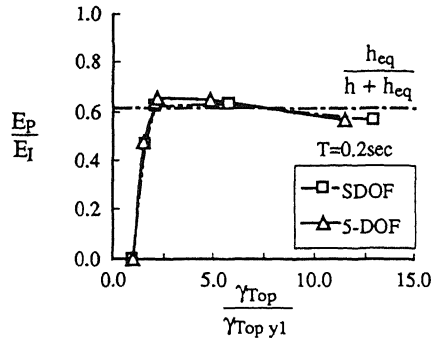

Fig. 14 Plastic dissipated energy ratios (5-DOF)

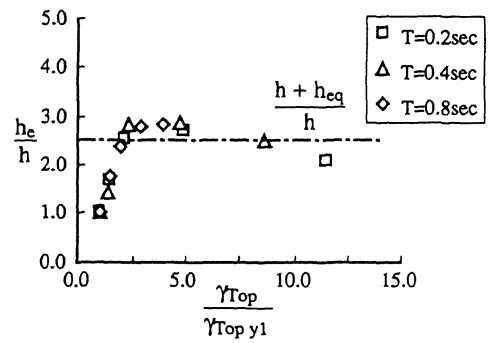

Fig. 15 Substitute damping ratios (5-DOF)

ACKNOWLEGEMENT

The authors wish to express their appreciation to S.Jidoh, S.Sugano, and T.Mochida of Takenaka Research Laboratory for their contribution to this study.

REFERENCES

Akiyama, H., Kato, B. 1975. Energy input and damages in structures subjected severe earthquakes: *Trans. of AIJ*:: No.235, 9-18.

Gulkan, P., Sozen, M.A. 1974. Inelastic response of reinforced concrete structures to earthquake motions: *Journal of ACI* : No.12, 604-610.

Inada, Y. 1987. Restoring force characteristic of reactor buildings based on load tests and numerical analysis: *Trans. of AIJ* : No.371, 61-71.

Jacobsen, L.S. 1960. Damping in composite structures: *Proc. 2nd WCEE* : 41.1-16. Tokyo.

Kibayashi, M. et al. 1981. Effects of plastic hysteresis models on earthquake responses: *Summaries of Tech. Papers AIJ* : 785-786.

Kibayashi, M., Hisatoku, T. 1988. Earthquake response analysis system of multi-D.O.F. structures: *Takenaka Tech. Research Report* : No.39, 67-81.

Setogawa, S , Yano, A. et al. 1988 Vibrational test of a model of nuclear power plant using a large shaking table (Part 1 and 2): *Proc. 9th WCEE* : VI.729-740.

Shiga, T. et al. 1974. Restoring force characteristics of reinforced concrete shear walls and earthquake responses: *Summaries of Tech. Papers AIJ* : 551-554.

Umemura, H. et al. 1973. *Dynamical aseismic design method of reinforced concrete structures*: 2.3, 304-307. Tokyo: Gihodo.